



Contents lists available at ScienceDirect

# Bioorganic & Medicinal Chemistry Letters

journal homepage: [www.elsevier.com/locate/bmcl](http://www.elsevier.com/locate/bmcl)

## Cyanoguanidine-based lactam derivatives as a novel class of orally bioavailable factor Xa inhibitors

Yan Shi <sup>\*</sup>, Jing Zhang <sup>†</sup>, Mengxiao Shi <sup>‡</sup>, Stephen P. O'Connor, Sharon N. Bisaha, Chi Li, Doree Sitkoff, Andrew T. Pudzianowski, Saeho Chong, Herbert E. Klei, Kevin Kish, Joseph Yanchunas Jr., Eddie C.-K. Liu, Karen S. Hartl, Steve M. Seiler, Thomas E. Steinbacher, William A. Schumacher, Karnail S. Atwal, Philip D. Stein

Research and Development, Bristol-Myers Squibb Company, PO Box 5400, Princeton, NJ 08543-5400, USA

### ARTICLE INFO

#### Article history:

Received 23 February 2009

Revised 5 June 2009

Accepted 8 June 2009

Available online 13 June 2009

#### Keywords:

Factor Xa inhibitor  
Cyanoguanidine  
Biosostere  
Thiourea  
Ketene aminal  
Bioavailable

### ABSTRACT

The *N,N'*-disubstituted cyanoguanidine is an excellent biosostere of the thiourea and ketene aminal functional groups. We report the design and synthesis of a novel class of cyanoguanidine-based lactam derivatives as potent and orally active FXa inhibitors. The SAR studies led to the discovery of compound **4** (BMS-269223,  $K_i = 6.5$  nM,  $EC_{2xPT} = 32$   $\mu$ M) as a selective, orally bioavailable FXa inhibitor with an excellent in vitro liability profile, favorable pharmacokinetics and pharmacodynamics in animal models. The X-ray crystal structure of **4** bound in FXa is presented and key ligand–protein interactions are discussed.

© 2009 Elsevier Ltd. All rights reserved.

The trypsin-like serine protease factor Xa (FXa) has been one of the major targets for antithrombotic agent development for some time.<sup>1</sup> Within the blood coagulation cascade, factor Xa functions at the point where the intrinsic and extrinsic coagulation pathways converge,<sup>2</sup> and FXa is the key enzyme responsible for thrombin activation. Thrombin plays a major role in thrombosis and hemostasis by mediating a feed-back loop that amplifies its production, inducing platelet aggregation and converting fibrinogen to fibrin which ultimately leads to clot formation. Selective FXa inhibitors are believed to have a wider therapeutic window than direct thrombin inhibitors, since FXa inhibition could significantly reduce thrombin generation and prevent thrombus formation, while the basal levels of thrombin would still facilitate hemostasis and reduce unwanted bleeding risk.<sup>2c</sup> Recent preclinical and clinical data indicate that selective inhibition of factor Xa is a highly effective approach to the prevention and treatment of arterial and venous thromboembolism.<sup>3</sup>

<sup>\*</sup> Corresponding author. Tel.: +1 609 818 4124; fax: +1 609 818 3450.

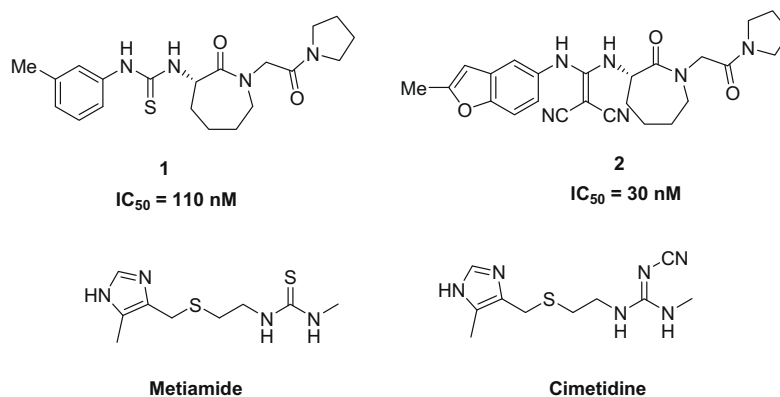
E-mail address: [yan.shi@bms.com](mailto:yan.shi@bms.com) (Y. Shi).

<sup>†</sup> Present address: Hoffman-La Roche Inc., 340 Kingsland Street, Nutley, NJ 07110, USA.

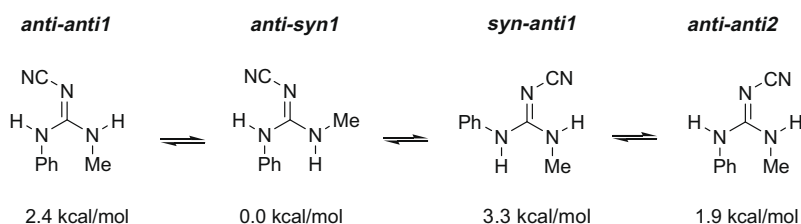
<sup>‡</sup> Present address: Wyeth Research, 401 N Middletown Road, Pearl River, NY 10965, USA.

Factor Xa contains a deep S1 cavity and a box-like S4 enclosure near the enzyme's active site. Potent FXa inhibitors generally require an S1 and an S4 binding element which are connected through an L-shaped scaffold. We have previously disclosed a series of caprolactam-based FXa inhibitors containing a thiourea **1**<sup>4</sup> or a ketene aminal **2**<sup>5</sup> as linkers of the P1 and P4 pharmacophores. While these compounds are selective and orally active FXa inhibitors, their in vivo efficacy was limited by their moderate in vitro potencies and short plasma half lives. In this Letter, we describe the cyanoguanidine as an alternative biosostere to the thiourea and ketene aminal motifs that can adopt the desired L-shaped conformation, and the detailed SAR studies of both P1 and P4 groups. The X-ray structure of compound **4** (BMS-269223) bound to FXa and the detailed analysis of its interactions with FXa, as well as the PK/PD data and in vivo pharmacology of compound **4**, will also be discussed.

The *N,N'*-disubstituted cyanoguanidine is known to be an excellent biosostere of *N,N'*-disubstituted thiourea from previous SAR studies of histamine H<sub>2</sub>-receptor antagonists.<sup>6</sup> For example, the cynaoguanidine moiety in Cimetidine is a biosostere of the thiourea functional group in Metiamide<sup>6a</sup> (Scheme 1). Similar to its thiourea and 1-nitroketene aminal analogs<sup>4,5</sup>, the 1-methyl-3-phenyl-2-cyanoguanidine (compound **3**) is predicted to prefer the *anti-syn1* conformation by gas phase ab initio calculations.<sup>7</sup>



**Scheme 1.** The thiourea **1**, ketene aminal **2**, Metiamide and Cimetidine.



**Scheme 2.** Relative energies of conformers of 1-methyl-3-phenyl-2-cyanoguanidine **3**.

**Scheme 2** shows the four lowest energy conformers for **3**. The other possible conformers are disfavored due to the internal steric interactions between the nitrogen substituents and the cyano group. The *anti-syn1* conformation affords the best combination of relief from steric crowding between the cyano, the phenyl and methyl groups.

Replacement of the 1,1-dicyanoketene aminal functionality in **2** with a cyanoguanidine gave compound **4** with an  $IC_{50}$  of 12 nM against FXa and  $EC_{2xPT}$  of 30  $\mu$ M (**Table 1**).<sup>8</sup> This compound is about threefold more potent than **2** ( $IC_{50}$  = 30 nM), indicating that both compounds likely adopt similar conformations when bound to FXa, and that the cyanoguanidine may even be a better linker than the ketene aminal in **2**. Similar SARs are observed for both series when the P1 group is a mono- or disubstituted phenyl group (data not shown).<sup>5</sup> In addition, analogs with a P1 group derived from alkylamines were uniformly poor FXa inhibitors, similar to results found in the thiourea series (data not shown).<sup>4</sup> Thus, we focused our efforts in SAR optimization on compound **4**.

Early efforts were concentrated on the possible isosteres of the 2-methylbenzofuran-7-yl pharmacophore to improve the potency. All efforts to replace the 2-methylbenzofuran with other bicyclic aryls resulted in significant losses in activity (**Table 1**). For example, the 2-naphthyl analog (**5**,  $IC_{50}$  = 780 nM) is about 60-fold less potent than **4**; replacement of the oxygen atom in 2-methyl benzofuran with either a sulfur (**6**,  $IC_{50}$  = 2882 nM) or NH (**10**,  $IC_{50}$  > 34,000 nM) led to analogs with much poorer activity compared to **4**. The isomeric 2-methylbenzofuran-6-yl analog **7** is completely inactive; while changing the 3-CH in the furan ring to a nitrogen atom led to compound **8** ( $IC_{50}$  = 2677 nM) with a 223-fold loss of activity. Other isosteric heteroaryl replacements (compounds **11–14**) are much less potent than **4**.

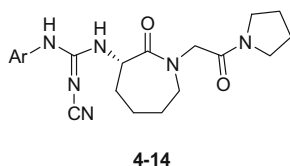
We next studied the SAR of substitutions on the 2-methyl benzofuran pharmacophore. Most changes to the substitution pattern on the furan ring resulted in significant losses in activity (**Table 2**). For example, the analog without the 2-methyl substituent (**15**,

$IC_{50}$  = 84 nM) is sevenfold less potent than **4**, while increasing the size of the 2-substituent from methyl to ethyl, resulted in a loss in activity of >1000-fold (**16**,  $IC_{50}$  = 15,538 nM). Changing the 2-methyl- to a 2-cyano-benzofuran led to a 20-fold less active compound **17** ( $IC_{50}$  = 2600 nM), while relocating the methyl group to the 3 position resulted in a 245-fold loss in activity (**18**,  $IC_{50}$  = 2939 nM). The 2,3-dimethyl substituted analog **19** is about 30-fold less active than **4**.

The SAR for the substituents of the phenyl ring of the 2-methyl benzofuran was also explored. While the 7-fluoro-2-methyl benzofuran analog (**20**,  $IC_{50}$  = 11 nM) has similar anti-FXa activity as compound **4**, both the 4- and 6-fluoro analogs (**21** and **22**) are less active. Increasing the size of the 7-substituent beyond a fluorine atom also produced less active compounds, with the 7-Cl (**23**) and 7-methyl (**24**) analogs showing about twofold loss of activity compared to **4**. Incorporation of bulkier 7-trifluoromethyl (**25**) and 7-methoxy (**26**) substituents led to significant losses of activity.

We also studied the SAR of the central caprolactam ring by varying its ring size and the chirality of its amino group. The results are summarized in **Table 3**. Compound **4**, the *S*-enantiomer with a seven-membered lactam ring, is the most potent analog among these compounds. It is about 77-fold more potent than its *R*-enantiomer **30** ( $IC_{50}$  = 940 nM) and the corresponding (*S*)-six-membered valerolactam analog **29** ( $IC_{50}$  = 928 nM). Both enantiomers of the five-membered lactam are very weak inhibitors of FXa. The racemic form of the eight-membered lactam analog **31** is also less potent than **4** with an  $IC_{50}$  of 195 nM.

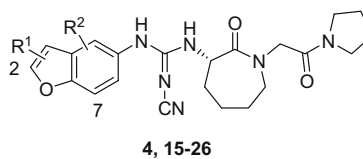
With the optimized P1 pharmacophore and central lactam ring in hand, we next turned our attention to the SAR studies of the P4 binding groups. Similar to the thiourea series,<sup>4</sup> the replacement of the pyrrolidine with non-cyclic amines, or modest changes to the ring size (azetidine and piperidine) led to significant losses in potency (data not shown). Substitutions at the C-2 and C-3 positions on the pyrrolidine ring were well tolerated but none of these ana-

**Table 1**  
SAR of the aromatic binding element

Compound	Ar	IC <sub>50</sub> (nM) <sup>a</sup>
<b>4</b>		12
<b>5</b>		780
<b>6</b>		2882
<b>7</b>		>34,000
<b>8</b>		2677
<b>9</b>		18,759
<b>10</b>		>34,000
<b>11</b>		11,879
<b>12</b>		>34,000
<b>13</b>		1300
<b>14</b>		2400

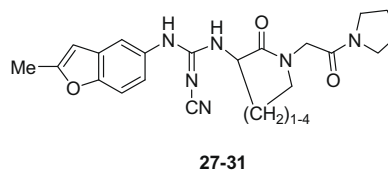
<sup>a</sup> IC<sub>50</sub>'s are measured against human factor Xa utilizing the cleavage of a synthetic substrate S-2222. Data are the average of two independent determinations.

logs were significantly more potent than the unsubstituted analog **4**. For example, compound **32** with a cyclopropane fused to the pyrrolidine has a similar IC<sub>50</sub> (15 nM) to **4** but with a weaker EC<sub>2xPT</sub> (56 μM). The 2-benzyl substituted pyrrolidine **33** (IC<sub>50</sub> = 19 nM) is slightly more potent than the 3-substituted analog **34** (IC<sub>50</sub> = 53 nM), but both show diminished EC<sub>2xPT</sub> (>50 μM).<sup>9</sup> Among the 2-aminomethyl substituted pyrrolidine analogs **35–38**, the R-enantiomers **36** and **38** are more potent than their S-enantiomers **35** and **37**, although the magnitude of difference is less dramatic in the **37/38** than in the **35/36** pair. Finally, the bicyclic analog **39**, which replaces the pyrrolidine in **4** with a 3,8-diazabicyclo[3.2.1]octane, provides the only compound more potent than **4** in this series with an IC<sub>50</sub> of 5 nM and EC<sub>2xPT</sub> of 11.5 μM.<sup>10</sup>

**Table 2**  
SAR of the substituted benzofurans

Compound	R <sup>1</sup>	R <sup>2</sup>	IC <sub>50</sub> (nM) <sup>a</sup>
<b>4</b>	2-H	H	12
<b>15</b>	2-Me	H	84
<b>16</b>	2-Et	H	15,538
<b>17</b>	2-CN	H	2600
<b>18</b>	2-Me	H	2939
<b>19</b>	2,3-Dimethyl	H	349
<b>20</b>	2-Me	7-F	11
<b>21</b>	2-Me	4-F	2728
<b>22</b>	2-Me	6-F	76
<b>23</b>	2-Me	7-Cl	27
<b>24</b>	2-Me	7-Me	21
<b>25</b>	2-Me	7-CF <sub>3</sub>	167
<b>26</b>	2-Me	7-OMe	14,818

<sup>a</sup> IC<sub>50</sub>'s are measured against human factor Xa utilizing the cleavage of a synthetic substrate S-2222. Data are the average of two independent determinations.

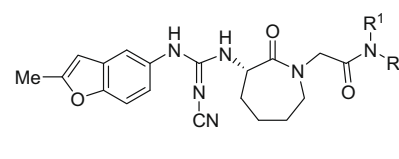
**Table 3**  
SAR of the central lactam core

Compound	Lactam core	IC <sub>50</sub> (nM) <sup>a</sup>
<b>27</b>		>32,000
<b>28</b>		30,000
<b>29</b>		928
<b>30</b>		940
<b>31</b>		195

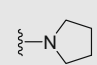
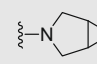
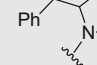
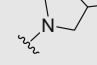
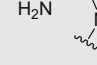
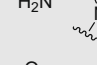
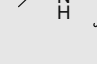
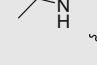
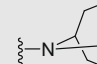
<sup>a</sup> IC<sub>50</sub>'s are measured against human factor Xa utilizing the cleavage of a synthetic substrate S-2222. Data are the average of two independent determinations.

The tight SAR observed for both the P1 and P4 binding pharmacophores can be rationalized by examining the X-ray crystal structure of compound **4** bound to FXa resolved at 2.2 Å shown in Figure 1.<sup>11</sup> As expected, the cyanoguanidine adopts the *anti-syn* conformation with the CN group positioned atop the disulfide bond. The central caprolactam carbonyl forms a hydrogen bond with NH of Gly216 (3.16 Å). The 2-methylbenzofuran moiety binds to FXa in the S1 pocket and the pyrrolidine is placed squarely in the S4 pocket.

**Table 4**  
SAR of the P4 binding pharmacophores



**4, 32–39**

Compound	NR <sup>1</sup> R <sup>2</sup>	IC <sub>50</sub> (nM) <sup>a</sup>	EC <sub>2×PT</sub> <sup>b</sup>
<b>4</b>		12	30
<b>32</b>		15	56
<b>33</b>		19	>50
<b>34</b>		53	>50
<b>35</b>		386	—
<b>36</b>		22	27
<b>37</b>		54	>50
<b>38</b>		28	33
<b>39</b>		5	11.5

<sup>a</sup> IC<sub>50</sub>'s are measured against Human Factor Xa utilizing the cleavage of a synthetic substrate S-2222.

<sup>b</sup> Concentration of inhibitor required to double the prothrombin based clotting time in human plasma. Data are the average of two independent determinations.

Figure 2a shows the detail of the S1 binding pocket with the favorable interaction volume, calculated by a GRID methyl probe in the absence of **4**.<sup>12</sup> The 2-methyl substituent of the benzofuran occupies the pocket at the base of S1, and there appears to be little room for increasing the size of this substituent; this correlates with the loss in activity seen for the 2-ethylbenzofuran compound **16**. Substitutions at other positions of the benzofuran were also found to be detrimental for the most part, in accordance with the view shown in Figure 2a. One exception is that small substituents at position 7 were tolerated (compounds **20**, **23**, **24**), in contrast to the expectation based on the apparent tight fit of 2-methyl benzofuran to the favorable interaction volume at this position. Position 7 is directed at the Ser195 side chain, which has been observed in some crystal structures to rotate and free up space for slightly larger ligands;<sup>8</sup> this may explain the tolerance for slight increases in the size of the 7-substituent. The contoured space near C6 in Figure

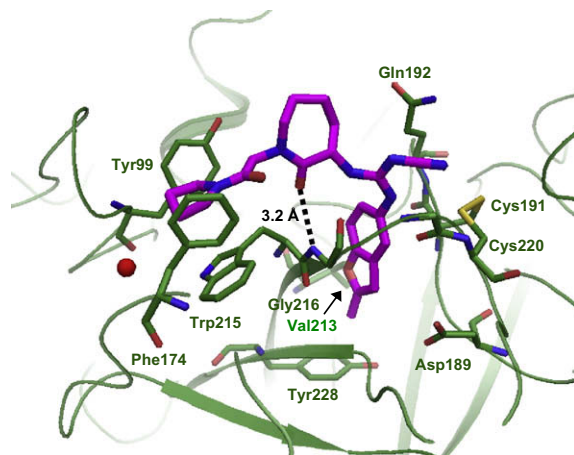
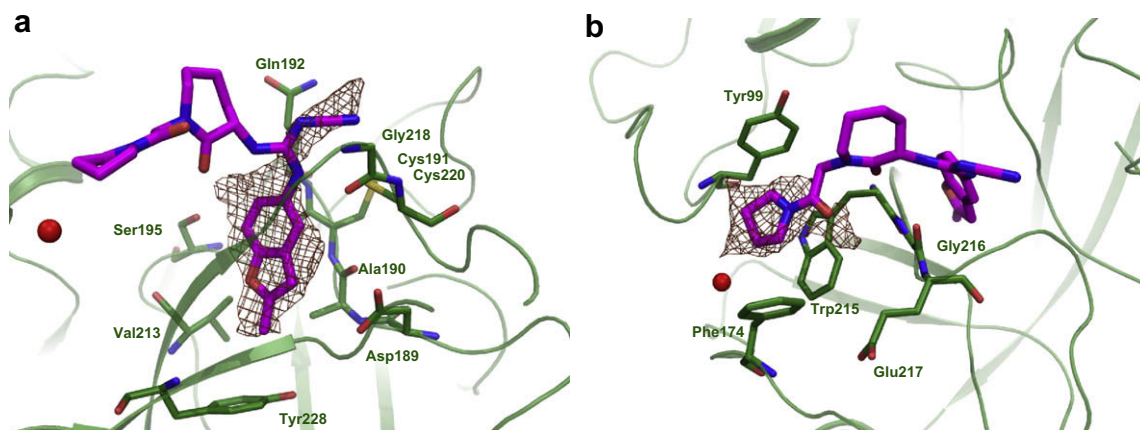


**Figure 1.** Crystal structure of **4** bound in FXa. The hydrogen bond between the ligand's lactam carbonyl and Gly216 backbone amide NH is highlighted. The conserved crystallographic water molecule in the far end of the P4 pocket is shown (red sphere). This and the following figures were created using PyMOL (<http://www.pymol.org>).

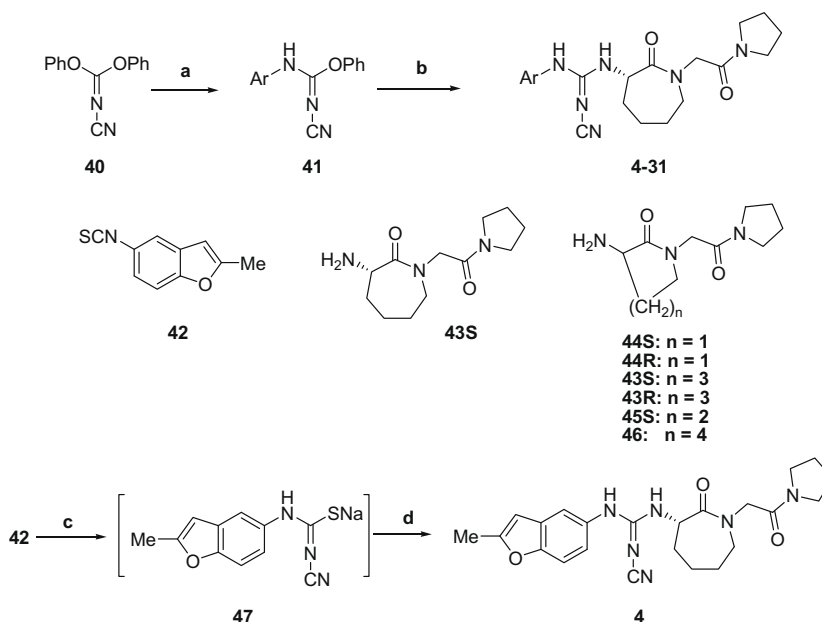
2a is actually above, rather than in the plane of the 2-methyl benzofuran ring, correlating with the reduced activity of **22**. The losses in activity seen in the 2-methylbenzofuran isosteres in Table 1 (compounds **6–14**) can also be understood to some degree by examining the crystal structure. The 2-methylbenzofuran pharmacophore is likely favored due to two attributes in addition to the space-filling nature of its shape: (1) it is overall relatively hydrophobic; (2) the slight polarization of the 2-methylbenzofuran ring is such that C3 is likely to have a small net partial positive charge due to the furan oxygen, allowing the 3-CH to interact favorably with Asp189. All of the isosteres differ in either one or both of these attributes.

Figure 2b shows the detail of the S4 binding pocket with the favorable interaction volume, calculated by a GRID methyl probe in the absence of **4**.<sup>12</sup> The carbonyl group of the pyrrolidine fills a pocket lined by the aliphatic portion of the side chain of Glu217. The pyrrolidine itself has a complementary shape to the favorable interaction volume, correlating with the observed difficulties in further optimizing this group. The single compound (**39**) showing an improvement in activity over compound **4**, may have a P4 group that augments the pyrrolidine-S4 shape complementarity with favorable electrostatic interactions between the ligand's charged NH and several potential partners near the S4 binding pocket, namely the backbone carbonyls of Thr97 or Glu98, or the conserved S4 water molecule, or some combination thereof; such interactions are seen in multiple examples of FXa-ligand crystal structures in the Protein Data Bank.<sup>13</sup>

Cyanoguanidines **4–31** were synthesized by the stepwise displacement of both phenoxy groups of diphenyl cyanocarbonimide **40** as shown in Scheme 3. Alternatively, compound **4** can also be prepared in a one-pot sequence according to a literature procedure.<sup>14</sup> Treatment of the 2-methyl benzofuran-7-isothiocyanate **42**<sup>5</sup> with sodium cyanoamide gave the intermediate **47**, which was reacted with caprolactam amine **43S**<sup>4</sup> and EDCI to afford **4** in 90% yield. Compounds **32–39** were prepared from the common intermediate acid **50** according to Scheme 4. Reaction of **47** and amine **48** with the assistance of EDCI provided methyl ester **49**. Hydrolysis of **49** afforded the acid **50**, which is then coupled with amines to produce **32–34** and BOC protected compounds **51a**, **51b**, and **52**. Compounds **51a**, **51b** and **52** were treated with TFA to yield **35**, **36** and **39**. Acetylation of **35** and **36** with acetic anhydride and triethylamine furnished **37** and **38**, respectively (Table 4).



**Figure 2.** Views of the (a) S1 and (b) S4 pockets of the FXa crystal structure complex with **4**. Available favorable interaction volumes, calculated with a GRID<sup>15</sup> methyl probe in the absence of **4**, are shown in brown contours (mapped at interaction level of  $-2.5$  kcal/mol).



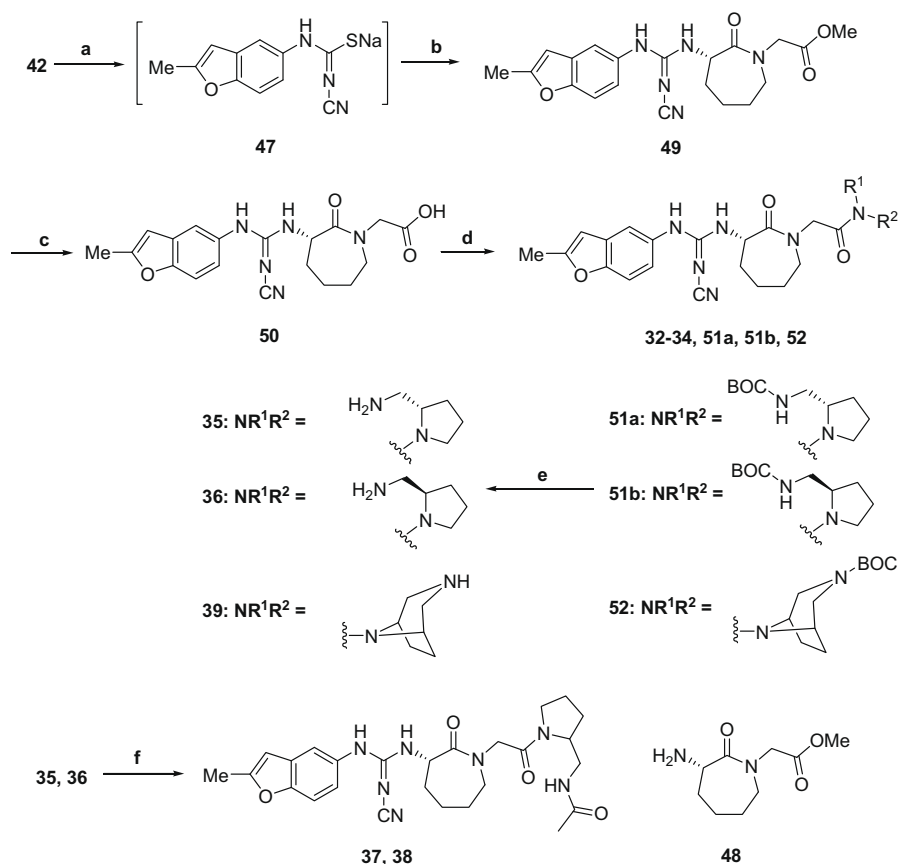
**Scheme 3.** The synthesis of **4-31**. Reagents and conditions: (a)  $ArNH_2$ ,  $CH_3CN$ ,  $80^\circ C$ ; (b) amine from **43** to **46**,  $80^\circ C$  (15–65% yield over two steps); (c) sodium cyanoamide, DMF  $60^\circ C$ ; (d) **43S**, 1-ethyl-3-[3-(dimethylamino)propyl]carbodiimide hydrochloride (EDCI) (90% yield).

Similar to the thiourea **1**<sup>4</sup> and ketene aminal **2**<sup>5</sup>, compound **4** is a selective FXa inhibitor relative to related trypsin-like serine proteases (570-fold vs t-PA and >1000-fold vs other serine proteases tested) as shown in Table 5. In addition, compound **4** is not a significant inhibitor of a panel human cytochrome P450 enzymes; it shows no significant activity in hERG, sodium channel, PXR and HHA assays.<sup>15</sup> It is negative in an Ames microbial mutagenicity study<sup>16</sup> up to  $400 \mu g/mL$ , and is inactive in an in vitro assessment of activity against 35 receptors and enzymes at  $10 \mu M$  (Cerep, Paris, France).<sup>17</sup> Furthermore, compound **4** exhibits good oral bioavailability in rats (50%), dogs (77%) and monkeys (49%). The terminal elimination half life ranged from 2.4 to 10.3 h and the volume of distribution was consistently low in preclinical animal models as shown in Table 6.

The anticoagulant and antithrombotic effects of **4** were determined in anesthetized rats.<sup>18</sup> Compound **4** was administered as initial loading plus sustaining infusions (mg/kg + mg/kg/h) of

2 + 2, 5 + 5, 10 + 10 and 20 + 20 which produced dose-dependent prolongation of ex vivo prothrombin time (Fig. 3) and inhibition of vena cava and carotid artery thrombosis (Fig. 4). Compound **4** was more potent in the venous thrombosis model ( $ED_{50} = 6 \pm 1$  mg/kg total dose, Fig. 4a) compared to the arterial thrombosis model ( $ED_{50} = 25 \pm 5$  mg/kg total dose, Fig. 4b). Anti-thrombotic activity was also evidenced by improved blood flow in arterial thrombosis. Whereas a high proportion of arteries were occluded with vehicle treatment (13/14 rats), occlusion rates were significantly reduced at compound **4** dose levels of 5 + 5 (4/8 rats), 10 + 10 (1/8 rats) and 20 + 20 (0/8 rats), but not at the 2 + 2 dose level (9/9 rats).

Compound **4** was also effective in prolonging prothrombin time when administered as an intraduodenal injection (Fig. 5). A 30 mg/kg intraduodenal injection of BMS-269223 increased prothrombin time by a factor of  $\geq 1.8$  for up to 120 min. In comparison, the 10 mg/kg + 10 mg/kg/h intravenous infusion increased prothrom-



**Scheme 4.** The synthesis of cyanoguanidine **32–39**. Reagents and conditions: (a) sodium cyanamide, DMF, 60 °C; (b) **48**, 1-ethyl-3-[3-(dimethylamino)propyl]carbodiimide hydrochloride (EDCI), 90% yield; (c) LiOH·2H<sub>2</sub>O, THF–H<sub>2</sub>O 98% yield; (d) HNR<sup>1</sup>R<sup>2</sup>, EDCI, Et<sub>3</sub>N, CH<sub>2</sub>Cl<sub>2</sub>, (75–90% yield); (e) TFA, CH<sub>2</sub>Cl<sub>2</sub>, 80–98% yield; (f) acetic anhydride, Et<sub>3</sub>N, CH<sub>2</sub>Cl<sub>2</sub>, 50–85% yield.

**Table 5**  
Selectivity profile of **4**

Human enzyme	$K_i$ (nM) <sup>a</sup>
Factor Xa	6.5
Trypsin	>10,000
Thrombin	6600
Tryptase	>16,000
Activated protein C	>18,000
u-PA	>7800
Plasmin	>16,000
t-PA	3700

<sup>a</sup>  $K_i$ 's are calculated from the IC<sub>50</sub> values assuming competitive inhibition versus the low molecular weight synthetic substrates using the relationship,  $K_i = IC_{50} / (1 + [S]/K_m)$ , where  $S$  is the substrate concentration in the assay and  $K_m$  is the Michaelis constant for that substrate. Data are the average of two independent determinations.

**Table 6**  
Pharmacokinetic parameters for **4** ( $n = 3$ , fasted)<sup>a</sup>

Parameter (unit)	Rat	Dog	Monkey
iv Dose (mg/kg)	7	8.3	10
CL <sub>total</sub> (L/kg)	1.7	0.12	2.2
$V_{dss}$ (L/kg)	0.19	0.11	1.8
$t_{1/2}$	2.4	10.3	2.9
MRT (h)	1.9	16	1.5
po Dose (mg/kg)	10	7	10
$C_{max}$	23	75	40
$T_{max}$	0.9	0.6	—
BA (%)	50	77	49

<sup>a</sup> Dosing vehicle: 10 mg/mL in PEG400/water (1:1, v/v).

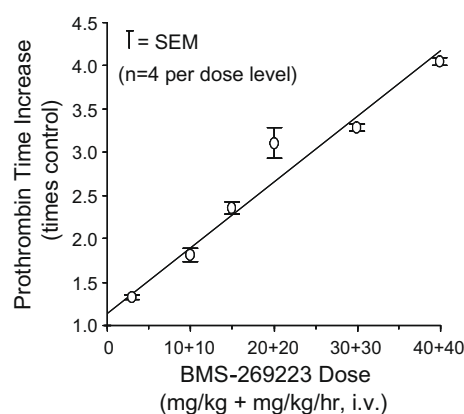


**Figure 3.** Prolongation of prothrombin time by intravenous infusion of **4** (BMS-269223).

bin time by a comparable factor of 1.8 and inhibited both venous and arterial thrombosis by  $\geq 50\%$ . This suggests that efficacy could also be achieved by oral dosing.

In summary, we have described a series of cyanoguanidine-based lactam derivatives as a novel class of orally bioavailable FXa inhibitors. The  $N,N'$ -disubstituted cyanoguanidines are excellent bioisosteres of their corresponding ketene aminal and thiourea functional groups. The SAR studies led to the discovery of compound **4** (BMS-269223) as a selective, orally bioavailable FXa inhibitor with an excellent in vitro liability profile, favorable pharmacokinetics and pharmacodynamics in animal models.

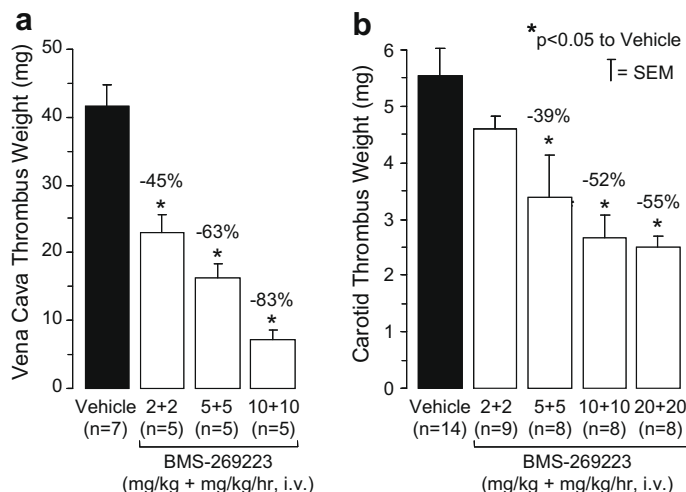


Figure 4. Inhibition of venous and arterial thrombosis by 4 (BMS-269223).

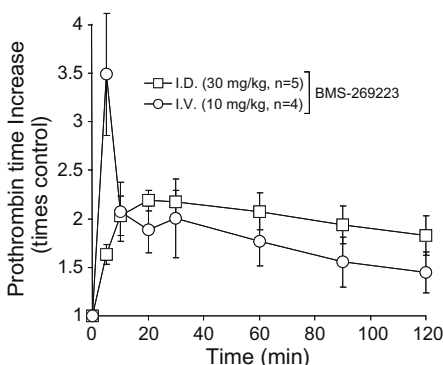


Figure 5. Prolongation of prothrombin time by intravenous and intraduodenal injection of 4 (BMS-269223).

## Acknowledgments

We thank Drs. P. T. Cheng, P. Y. S. Lam, R. R. Wexler for insightful review of this work.

## References and notes

- For reviews, see: (a) Kunitada, S.; Nagahara, T.; Hara, T. *Handbook Exp. Pharmacol.* **1998**, 397; (b) Vacca, J. P. *Ann. Rev. Med. Chem.* **1998**, 33, 81; (c) Zhu, B.-Y.; Scarborough, R. M. *Curr. Opin. Cardiovasc., Pulmon., Ren. Invest. Drugs* **1999**, 1, 63; (d) Ewing, W. R.; Pauls, H. W.; Spada, A. P. *Drugs Future* **1999**, 24, 771; (e) Fevig, J. M.; Wexler, R. R. *Ann. Rev. Med. Chem.* **1999**, 34, 81; (f) Betz, A. *Exp. Opin. Ther. Patent* **2001**, 11, 1007.
- (a) Davie, E. W.; Fujikawa, K.; Kistiel, W. *Biochemistry* **1991**, 30, 10363; (b) Butenas, S.; Van 't Veer, C.; Cawthorn, K.; Brummel, K. E.; Mann, K. G. *Blood Coagul. Fibrin.* **2000**, 11, S9; (c) Wong, P. C.; Watson, C. A.; Crain, E. J.; Ogletree, M. L.; Wexler, R. R.; Lam, P. Y. S.; Pinto, D. J.; Knabb, R. M. *J. Thromb. Haemost.* **2007**, 5, Abstr. 1315.
- For Apixaban, see: (a) Lassen, M. R.; Davidson, B. L.; Gallus, A.; Pineo, G.; Ansell, J.; Deitchman, D. J. *Thromb. Haemost.* **2007**, 5, 2368; (b) Pinto, D. J. P.; Orwat, M. J.; Koch, S.; Rossi, K. A.; Alexander, R. S.; Smallwood, A.; Wong, P. C.; Rendina, A. R.; Luettgen, J. M.; Knabb, R. M.; He, K.; Xin, B.; Wexler, R. R.; Lam, P. Y. S. *J. Med. Chem.* **2007**, 50, 5339; (c) Wong, P. C.; Crain, E. J.; Xin, B.; Wexler, R. R.; Lam, P. Y.; Pinto, D. J.; Luettgen, J. M.; Knabb, R. M. *J. Thromb. Haemost.* **2008**, 6, 820; For Rivaroxaban, see: (d) Roehrig, S.; Straub, A.; Pohlmann, J.; Lampe, T.; Pernerstorfer, J.; Schlemmer, K.-H.; Reinemer, P.; Perzborn, E. *J. Med. Chem.* **2005**, 48, 5900; (e) Eriksson, B. I.; Borris, L.; Dahl, O. E.; Haas, S.; Huisman, M. V.; Kakkar, A. K.; Misselwitz, F.; Kaelebo, P. *J. Thromb. Haemost.* **2006**, 4, 121; (f) Kubitz, D.; Becka, M.; Wensing, G.; Voith, B.; Zuehlsdorf, M. *Eur. J. Clin. Pharmacol.* **2005**, 61, 873; (g) Turpie, A. G. G.; Fisher, W. D.; Bauer, K. A.; Kwong, L. M.; Irwin, M. W.; Kalebo, P.; Misselwitz, F.; Gent, M. *J. Thromb. Haemost.* **2005**, 3, 2479; For LY517717, see: (h) Agnelli, G.; Haas, S. K.; Krueger, K. A.; Bedding,

- A. W.; Brandt, J. T. *ASH Ann. Meet. Abstr.* **2005**, 106, 278; (i) Hampton, T. *JAMA J. Am. Med. Assoc.* **2006**, 295, 743; (j) Liebeschuetz, J. W.; Jones, S. D.; Wiley, M. E.; Young, S. C. *Struct.-Based Drug Discovery* **2006**, 173.
- Bisacchi, G. S.; Stein, P. D.; Gougoutas, J. Z.; Hartl, K. S.; Lawrence, R. M.; Liu, E. C.; Pudzianowski, A. T.; Schumacher, W. A.; Sitkoff, D.; Steinbacher, T. E.; Sutton, J.; Zhang, Z.; Seiler, S. M. *Lett. Drug Des. Discovery* **2005**, 2, 625.
- Shi, Y.; Zhang, J.; Stein, P. D.; Shi, M.; O'Connor, S. P.; Bisaha, S. N.; Li, C.; Atwal, K. S.; Bisacchi, G. S.; Sitkoff, D.; Pudzianowski, A. T.; Liu, E. C.; Hartl, K. S.; Seiler, S. M.; Youssef, S.; Steinbacher, T. E.; Schumacher, W. A.; Rendina, A. R.; Bozarth, J. M.; Peterson, T. L.; Zhang, G.; Zahler, R. *Bioorg. Med. Chem. Lett.* **2005**, 15, 5453.
- (a) Silverman, R. B. In *The Organic Chemistry of Drug Design and Drug Action*; Academic: New York, 1992; pp 159–165; (b) Durant, G. J.; Emmett, J. C.; Ganellin, C. R.; Miles, P. D.; Parsons, M. E.; Prain, H. D.; White, G. R. *J. Med. Chem.* **1977**, 20, 901; (c) Black, J. W.; Durant, G. J.; Ganellin, C. R. *Nature* **1974**, 248, 65; (d) Bradshaw, J. C.; Ganellin, C. R.; Parsons, M. E. *J. Int. Med. Res.* **1975**, 3, 86; (e) Domschke, W.; Lux, G.; Domschke, D. *Lancet* **1979**, 8111, 320.
- All calculations were done at the RI-MP2/6-31+G(d,p) level of theory with the q-CHEM 3.0 program system: (a) Feyereisen, M.; Fitzgerald, G.; Komornicki, A. *Chem. Phys. Lett.* **1993**, 208, 359; (b) Shao, Y.; Fusti-Molnar, L.; Jung, Y.; Kussmann, J.; Ochsenfeld, C.; Brown, S. T.; Gilbert, A. T. B.; Slipchenko, L. V.; Levchenko, S. V.; O'Neill, D. P.; Distasio, R. A. Jr.; Lochan, R. C.; Wang, T.; Beran, G. J. O.; Besley, N. A.; Herbert, J. M.; Lin, C. Y.; Van Voorhis, T.; Chien, S. H.; Sodt, A.; Steele, R. P.; Rassolov, V. A.; Maslen, P. E.; Korambath, P. P.; Adamson, R. D.; Austin, B.; Baker, J.; Byrd, E. F. C.; Datchsel, H.; Doerksen, R. J.; Dreuw, A.; Dunietz, B. D.; Dutoi, A. D.; Furlani, T. R.; Gwaltney, S. R.; Heyden, A.; Hirata, S.; Hsu, C.-P.; Kedziora, G.; Khalliulin, R. Z.; Klunzinger, P.; Lee, A. M.; Lee, M. S.; Liang, W.; Lotan, I.; Nair, N.; Peters, B.; Proynov, E. I.; Pieniazek, P. A.; Rhee, Y. M.; Ritchie, J.; Rosta, E.; Sherrill, C. D.; Simmonett, A. C.; Subotnik, J. E.; Woodcock, H. L. III; Zhang, W.; Bell, A. T.; Chakraborty, A. K.; Chipman, D. M.; Keil, F. J.; Warshel, A.; Hehre, W. J.; Schaefer III, H. F.; Kong, J.; Krylov, A. I.; Gill, P. M. W.; Head-Gordon, M. *Phys. Chem. Chem. Phys.* **2006**, 8, 3172.
- For detailed assay methods, see: Shi, Y.; Sitkoff, D.; Zhang, J.; Klei, H. E.; Kish, K.; Liu, E. C.-K.; Hartl, K. S.; Seiler, S. M.; Chang, M.; Huang, C.; Youssef, S.; Steinbacher, T. E.; Schumacher, W. A.; Grazier, N.; Pudzianowski, A.; Apedo, A.; Disenza, L.; Yanchunas, J., Jr.; Stein, P. D.; Atwal, K. S. *J. Med. Chem.* **2008**, 51, 7541.
- Several literature reports suggest that highly nonpolar coagulation factor inhibitors can have a tendency toward high protein binding, and this tendency could be associated with the relatively high concentrations required to achieve efficacy in plasma-based assays and presumably in vivo. Most of compounds in this series have the concentrations to double the prothrombin time ( $EC_{2 \times PT}$ ) on the order of  $10^3$  times higher than the corresponding  $IC_{50}$ 's probably due to plasma protein binding. For example, compound 4 is 98.7% plasma protein bound in human plasma. See Ref. 8.
- Compound 39 was synthesized much later after the discovery of compound 4, and it was not fully characterized in vivo.
- The X-ray crystal structure coordinates of 4 in human factor Xa have been deposited in the Protein Data Bank (PDB code 3HPT).
- Contours calculated using GRID (version 22a, Molecular Discovery) with methyl probe C3, contoured at interaction energy level of  $-2.5$  kcal/mol: Goodford, P. J. *J. Med. Chem.* **1985**, 28, 849.
- Some examples are ascension codes 1lpk, 1nfu, 1nfy, 1xka, 1xkb, 1wu1, 2h9e.
- Atwal, K. S.; Ahmed, S. Z.; O'Reilly, B. C. *Tetrahedron Lett.* **1989**, 30, 7313.
- Compound 4 has following safety profile: CYP (inhibition) 3A4-BFC  $IC_{50}$  = 18.5  $\mu$ M, 2C9  $IC_{50}$  = 29.2  $\mu$ M, others (3A4-BZR, 1A2, 2B6, 2C8, 2C19, 2D6) all  $IC_{50}$ 's > 40  $\mu$ M; PXR  $EC_{50}$  > 25  $\mu$ M; hERG (flux)  $IC_{50}$  > 80  $\mu$ M; HHA (2C19, 2C9, 2D6, 3A4, TC5) all  $IC_{50}$ 's > 200  $\mu$ M. Spectral data for compound 4:  $^1H$  NMR (500 MHz,  $CDCl_3$ )  $\delta$  7.42 (d, 1H,  $J$  = 8.1 Hz), 7.32 (d, 1H,  $J$  = 2.2 Hz), 7.07–

- 7.03 (m, 2H), 6.46 (d, 1H,  $J = 5.5$  Hz), 6.38 (s, 1H), 4.61 (dd, 1H,  $J = 10.0, 5.5$  Hz), 4.13–4.03 (m, 2H), 3.72–3.65 (m, 1H), 3.43 (t, 2H,  $J = 7.15$  Hz), 3.37–3.30 (m, 2H), 3.24–3.19 (m, 1H), 2.46 (s, 3H), 2.18–2.12 (m, 1H), 2.0–1.92 (m, 3H), 1.84–1.71 (m, 5H), 1.57–1.49 (m, 1H) ppm; Anal. Calcd for  $C_{23}H_{28}N_6O_3$ : C, 62.74; H, 6.61; N, 18.76. Found: C, 62.89; H, 6.69; N, 18.55;  $t_R = 5.9$  min with the HPLC condition: Column-Zorbax SB C18  $4.6 \times 75$  mm; flow-2.5 mL/min detected at 220 nm; solvent A = 10%  $CH_3OH + 90\% H_2O + 0.2\% H_3PO_4$ , solvent B = 90%  $CH_3OH + 10\% H_2O + 0.2\% H_3PO_4$ ; gradient-linear, 50% A to 0% A over 8 min then hold.
16. Maron, D. M.; Ames, B. N. *Mutat. Res.* **1983**, 113, 173.
  17. Cerep in vitro pharmacology screening package including the following assays:  $A_1$  (h),  $\alpha_1$  (non-selective) (r),  $\alpha_2$  (non-selective) (r),  $\beta_1$  (h),  $\beta_2$  (h), BZD (central) (r), CCK<sub>A</sub> (CCK<sub>1</sub>) (h), D<sub>1</sub> (h), D<sub>2S</sub> (h), AMPA (r), Kainate (r), NMDA (r), H<sub>1</sub> (central) (guinea-pig), H<sub>2</sub> (guinea-pig), MAO-A (r), MAO-B (r), M (non-selective) (r), Opiate (non-selective) (r), PCP (r), Rolipram (m), 5-HT (non-selective) (r), 5-HT<sub>1A</sub> (h), 5-HT<sub>2B</sub> (h), sst (non-selective), GR (h), ER $\alpha$  (h), PR (h), Ca<sup>2+</sup> channel (L, DHP site) (r), Ca<sup>2+</sup> channel (L, verapamil site) (r), Na<sup>+</sup> channel (site 2) (r), Cl-channel (r), NE transporter (h), DA transporter (r), GABA transporter (r), Choline transporter (r). For details regarding the specific receptors and experimental conditions see: <http://www.cerep.fr/Cerep/Users/pages/catalog/binding/catalog.asp>.
  18. Arterial and venous thrombosis were performed in pentobarbital-anesthetized male Sprague Dawley rats as described in: Schumacher, W. A.; Heran, C. L.; Steinbacher, T. E. *J. Cardiovas. Pharmacol.* **1996**, 28, 19. To measure ex vivo clotting time, rats were fasted overnight and anesthetized with sodium pentobarbital (50 mg/kg, ip). Catheters were placed in a jugular vein for iv dosing, and into the duodenum at the level of the bile duct for intraduodenal dosing. Arterial blood samples were withdrawn from a carotid artery catheter into 3.8% Na-citrate (1/10; v/v) to measure prothrombin time by the standard procedure described for Dade Thromboplastin-C reagent (Baxter Healthcare Corp., Miami, FL) (Baxter Healthcare Corp., Miami, FL), which had an international sensitivity index of 2.0 for the mechanical clot detection method employed. The dosing solution for these studies was 10% ethanol/90% PEG300 in a volume of 1 mL/kg for bolus iv or intraduodenal dosing, and at 1 mL/kg/h for sustaining iv infusion.